
Enzyme immobilization on covalent organic framework supports

In the format provided by the authors and unedited

Enzyme Immobilization on Covalent Organic Framework Supports

Qianqian Zhu,^{#ab} Yunlong Zheng,^{#ac} Zhenjie Zhang^{*ab} and Yao Chen^{*ac}

^a State Key Laboratory of Medicinal Chemical biology, Nankai University, Tianjin 300071, P.R. China

^b College of Chemistry, Nankai University, Tianjin 300071, P.R. China

^c College of Pharmacy, Nankai University, Tianjin 300071, P.R. China

*Corresponding author: zhangzhenjie@nankai.edu.cn, chenyaoyao@nankai.edu.cn

Supplementary Figure 1 | FT-IR spectrums of BSA, BSA@ZPF-2, BSA@ZPF-2@COF-42-B and BSA@COF-42-B.

Supplementary Figure 2 | **(a)** N₂ adsorption isotherms and **(b)** pore size distribution calculated based on DFT method.

Supplementary Figure 3 | PXRD patterns of BSA@ZPF-2@COF-42-B with different etching time.

Supplementary Figure 4 | **(a)** PXRD patterns and **(b)** TEM images of BSA@ZIF-90@COF-43-B before and after etching.

Supplementary Figure 5 | Adsorption curve of COF-42-B for BSA.

Supplementary Figure 6 | The leakage test for CAT during the process of etching. The result revealed that there was negligible leakage during this process.

Supplementary Figure 7 | **(a)** Recycling experiments of CAT@COF-42-B. **(b)** The leakage of CAT@COF-42-B during 10 catalysis cycles.

Supplementary Figure 8 | Loading amounts **(a)** and leaking percentages **(b)** of immobilization systems in the experience.

Supplementary Figure 9 | Adsorption kinetic curve of Lipase@NKCOF-100 **(a)** and Lipase@ MCM-41 **(b)**

Supplementary Figure 10 | Confocal laser scanning microscopy (CLSM) of NKCOF-98 **(a)** and Lipase-FITC@NKCOF-98 prepared by physical adsorption **(b)**.

Supplementary Figure 11 | Energy dispersive spectrometer (EDS) element mapping

of NKCOF-98.

Supplementary Figure 12 | ^1H NMR spectra of aspirin methyl ester (AME) and the product of AME hydrolysis by Lipase@NKCOF-98.

Supplementary Figure 13 | ^1H NMR spectra of aspirin methyl ester (AME) and the product of AME hydrolysis by Lipase@NKCOF-99.

Supplementary Figure 14 | ^1H NMR spectra of aspirin methyl ester (AME) and the product of AME hydrolysis by Lipase@ZIF-8.

Supplementary Figure 15 | ^1H NMR spectra of aspirin methyl ester (AME) and the product of AME hydrolysis by Lipase@MCM-41.

Supplementary Figure 16 | ^1H NMR spectra of aspirin methyl ester (AME) and the product of AME hydrolysis by Lipase@NKCOF-100.

Supplementary Table 1 | Analytical conditions.

Supplementary Figure 17 | Catalytic reaction results (HPLC) of various Lipase@materials in the period of 12 h.

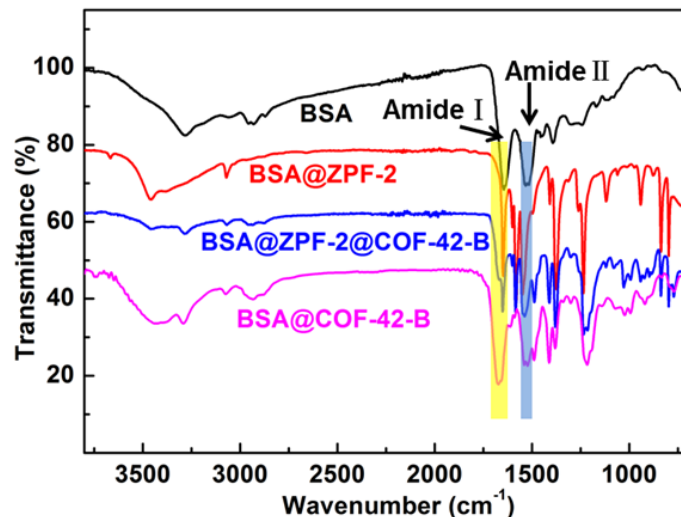
Supplementary Figure 18 | Catalytic reaction results (HPLC) of free lipase, Lipase@NKCOF-98 and Lipase@NKCOF-99 in chiral resolution of R, S-1-(p-tolyl)ethanol.

Supplementary Figure 19 | Catalytic reaction results (HPLC) of free lipase, Lipase@NKCOF-98 and Lipase@NKCOF-99 in chiral resolution of R, S-1-(4-fluorophenyl)ethanol.

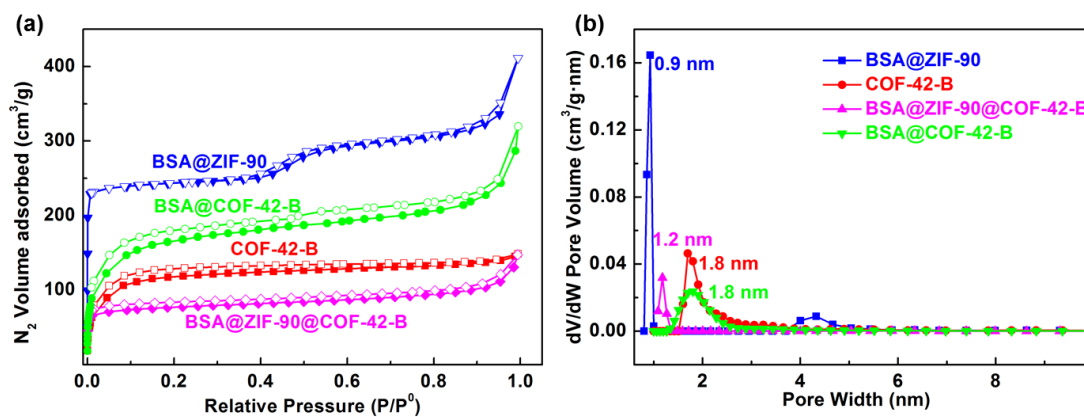
Supplementary Figure 20 | Catalytic reaction results (HPLC) of free lipase, Lipase@NKCOF-98 and Lipase@NKCOF-99 in chiral resolution of R, S-1-Phenyl-2-propanol.

Supplementary Figure 21 | Catalytic reaction results (HPLC) of free lipase, Lipase@NKCOF-98 and Lipase@NKCOF-99 in chiral resolution of R, S-1-Phenyl-1-propanol.

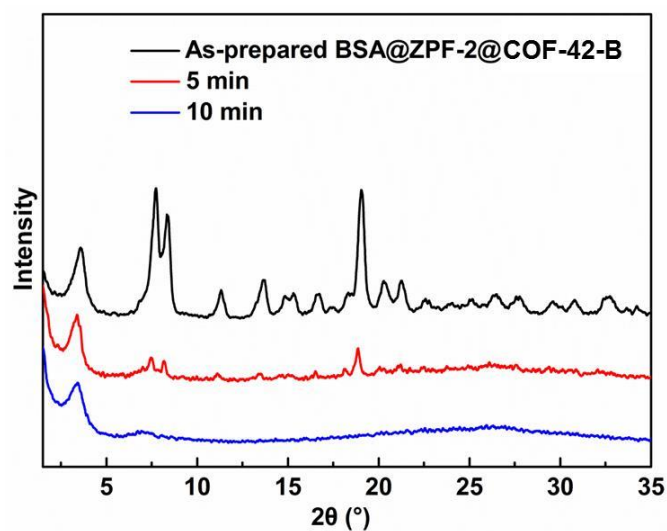
Supplementary Figure 22 | Catalytic reaction results (HPLC) of free lipase, Lipase@NKCOF-98 and Lipase@NKCOF-99 in chiral resolution of R, S-1-(1-Naphthyl)ethanol.



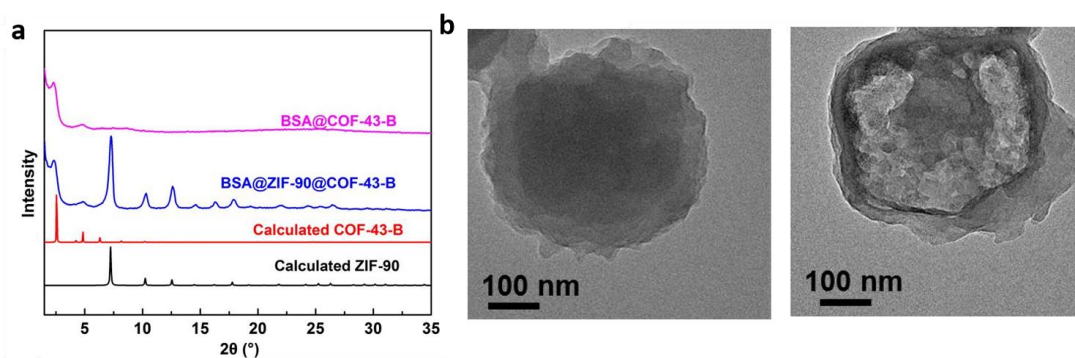
Supplementary Figure 1 | FT-IR spectrums of BSA, BSA@ZPF-2, BSA@ZPF-2@COF-42-B and BSA@COF-42-B. (amide I mainly from C=O stretching mode and II band mainly from a combination between of NH bending and CN stretching modes).



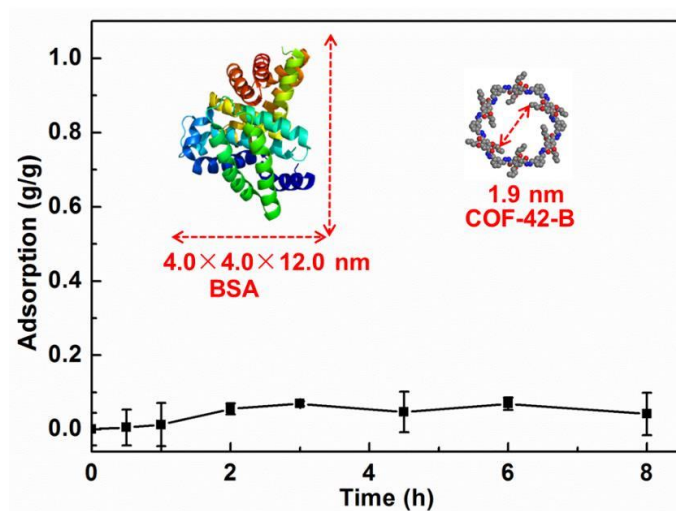
Supplementary Figure 2 | (a) N₂ adsorption isotherms and (b) pore size distribution calculated based on DFT method for BSA@ZIF-90 (blue), COF-42-B (red), BSA@ZIF-90@COF-42-B (purple) and BSA@COF-42-B (green).



Supplementary Figure 3 | PXRD patterns of BSA@ZPF-2@COF-42-B with different etching time.

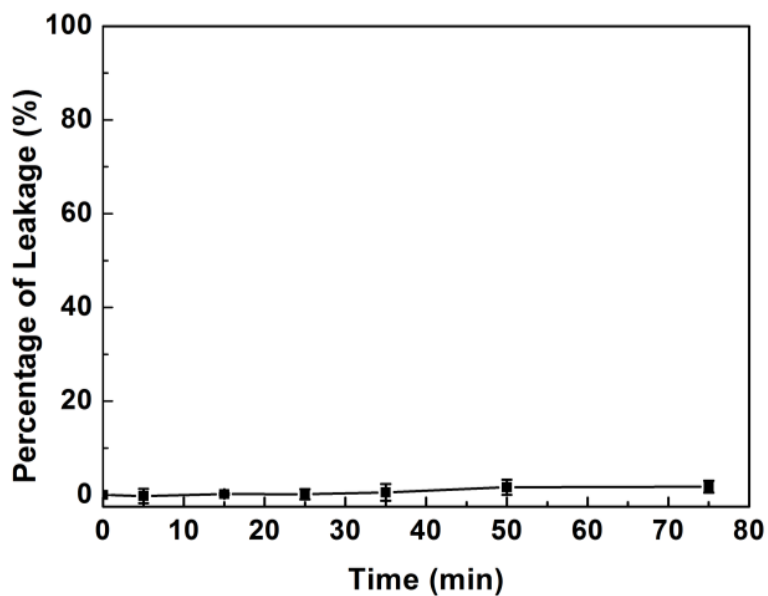


Supplementary Figure 4 | (a) PXRD patterns and (b) TEM images of BSA@ZIF-90@COF-43-B before and after etching.

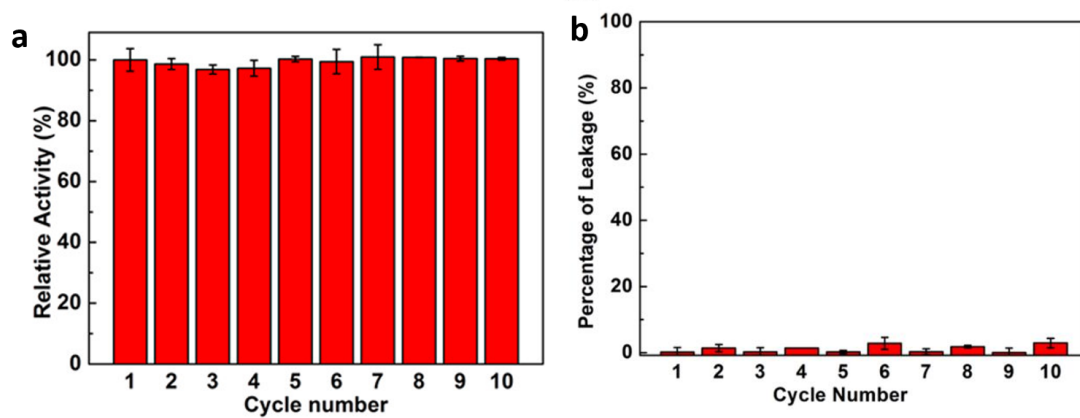


Supplementary Figure 5 | Adsorption curve of COF-42-B for BSA. Because the pore

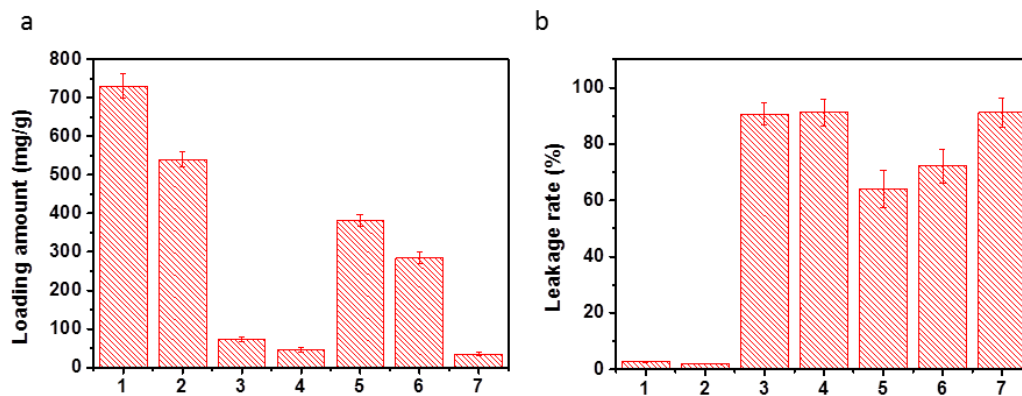
of COF-42-B is not big enough to accommodate BSA, there is almost no uptake observed for BSA.



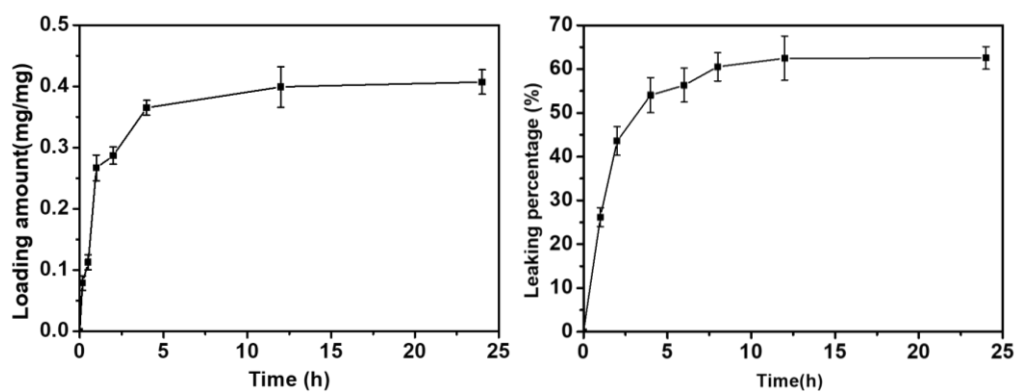
Supplementary Figure 6 | The leakage test for CAT during the process of etching. The result revealed that there was negligible leakage during this process.



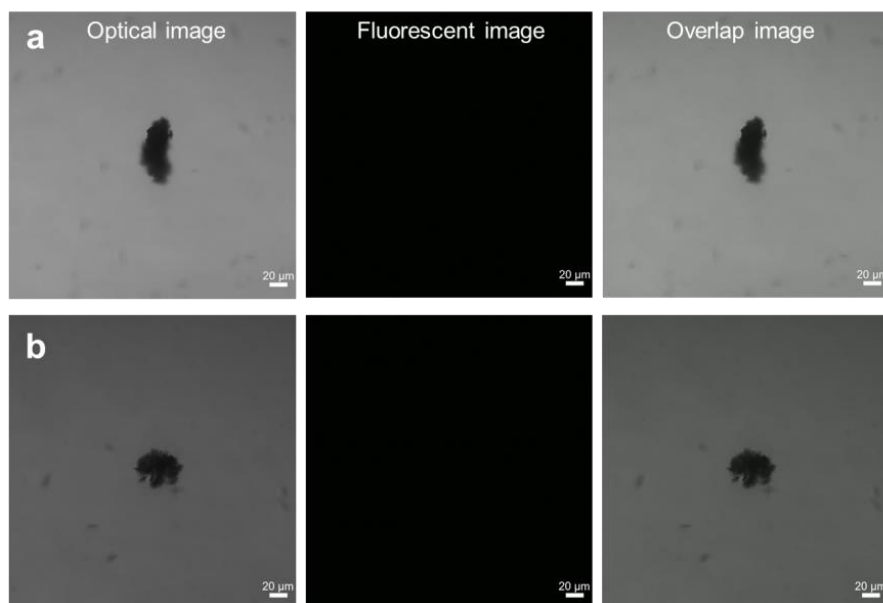
Supplementary Figure 7 | (a) Recycling experiments of CAT@COF-42-B. (b) The leakage of CAT@COF-42-B during 10 catalysis cycles.



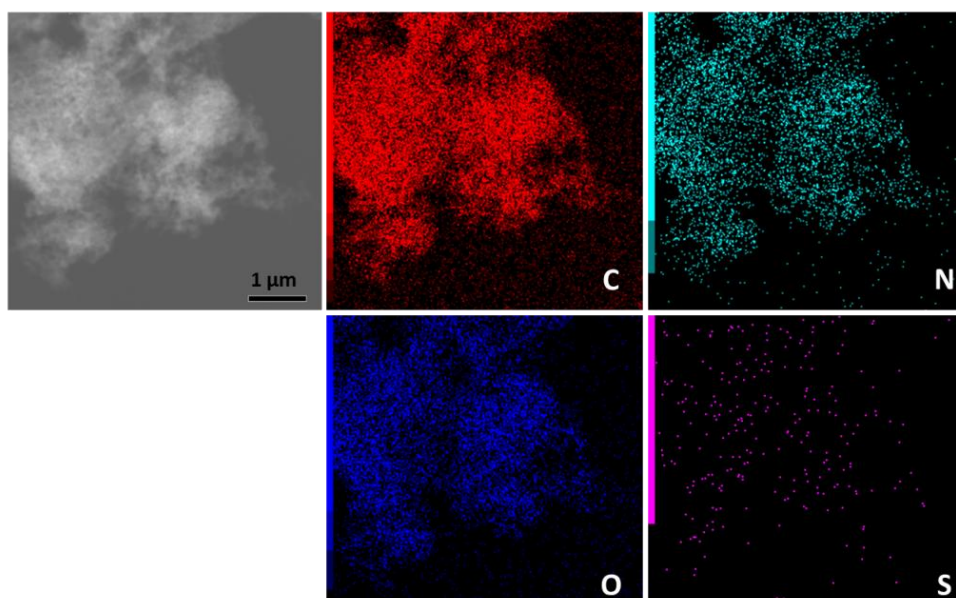
Supplementary Figure 8 | Loading amounts (a) and leaking percentages (b) of immobilization systems in the experience. (1) Lipase@NKCOF-98 (in-situ); (2) Lipase@NKCOF-99 (in-situ); (3) Lipase@NKCOF-98 (adsorption); (4) Lipase@NKCOF-99 (adsorption); (5) Lipase@NKCOF-100 (adsorption); (6) Lipase@MCM-41 (adsorption) and (7) Lipase@activated carbon (adsorption).



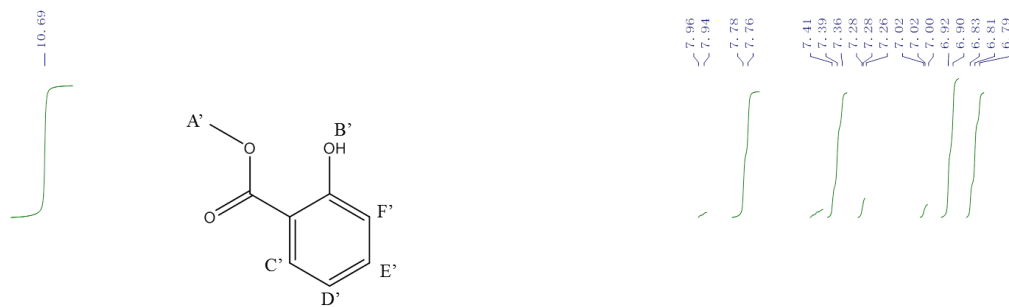
Supplementary Figure 9 | Adsorption kinetic curve of Lipase@NKCOF-100 (a) and Lipase@ MCM-41 (b).



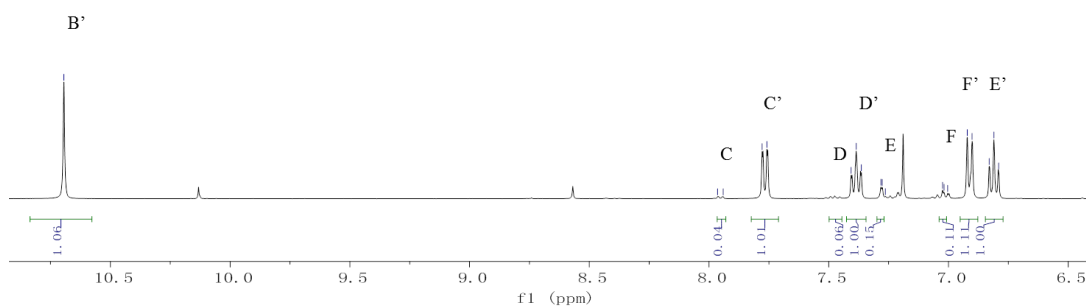
Supplementary Figure 10 | Confocal laser scanning microscopy (CLSM) of NKCOF-98 (a) and Lipase-FITC@NKCOF-98 prepared by physical adsorption (b).



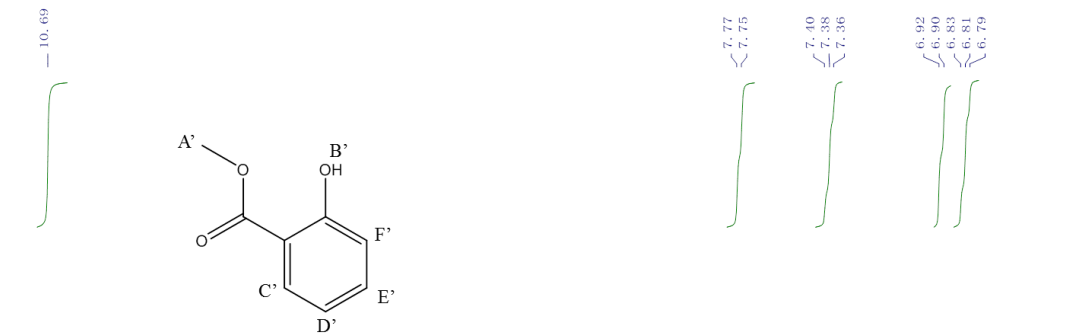
Supplementary Figure 11 | Energy dispersive spectrometer (EDS) element mapping of NKCOF-98.



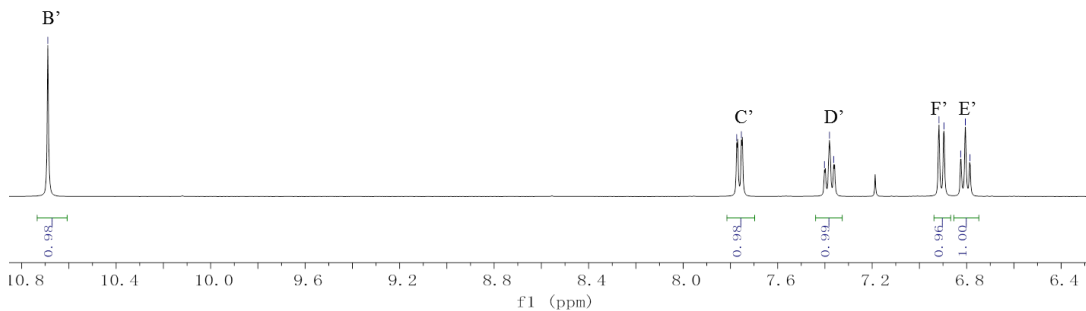
Conversion rate = $4.12 / 4.48 = 91.96\%$



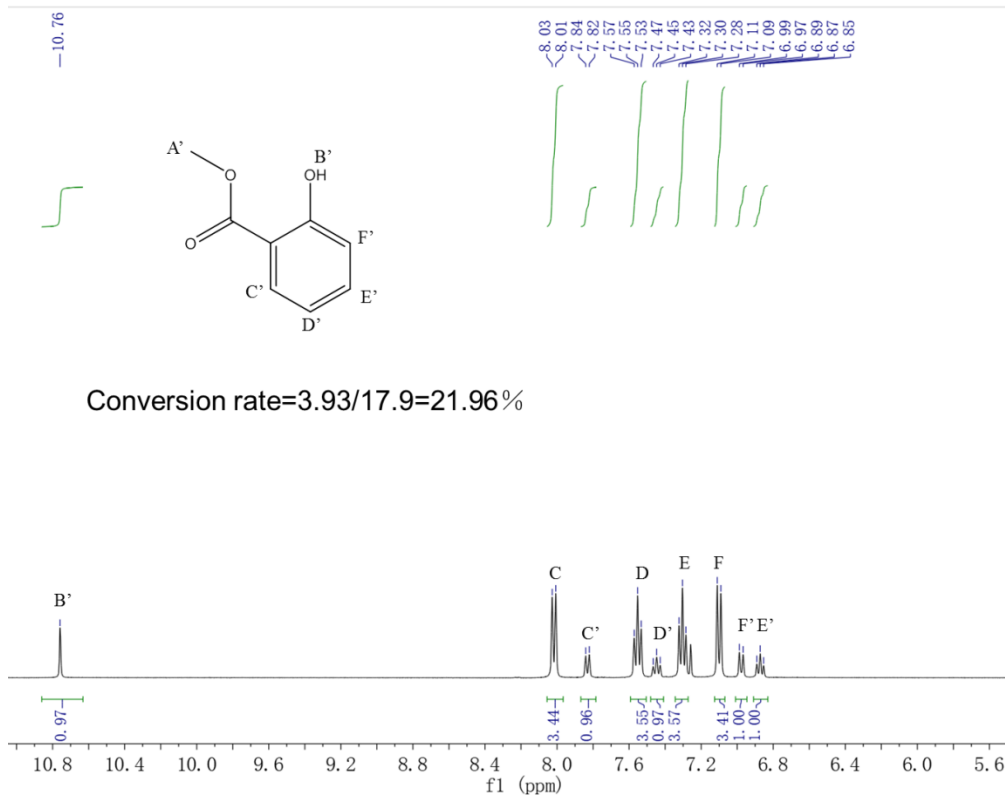
Supplementary Figure 12 | ¹H NMR spectra of aspirin methyl ester (AME) and the product of AME hydrolysis by Lipase@NKCOF-98.



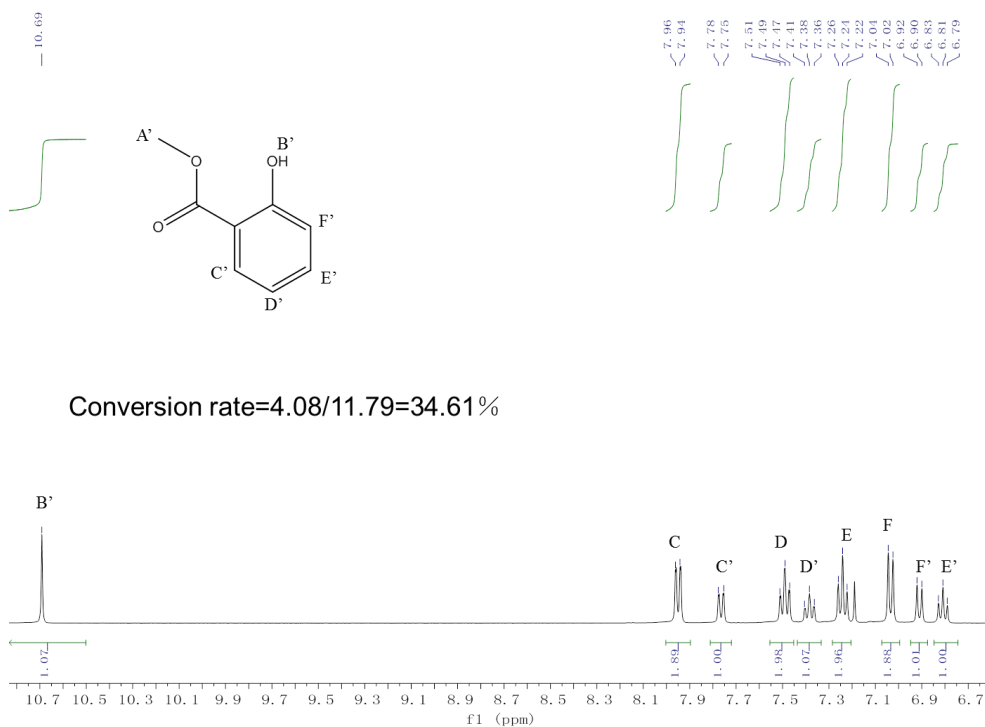
Conversion rate = 100%



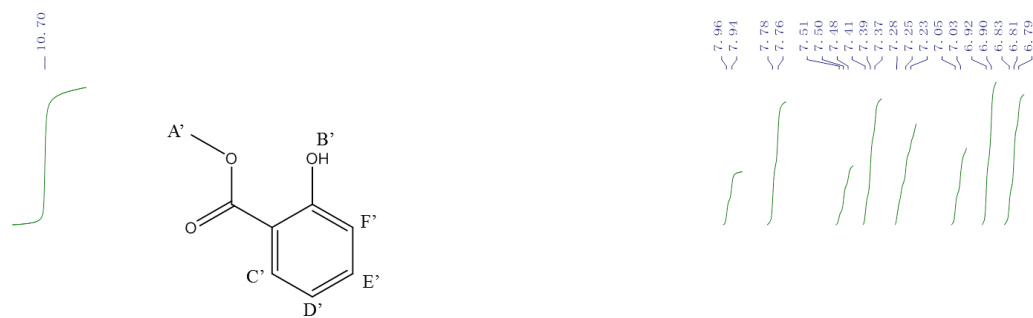
Supplementary Figure 13 | ¹H NMR spectra of aspirin methyl ester (AME) and the product of AME hydrolysis by Lipase@NKCOF-99.



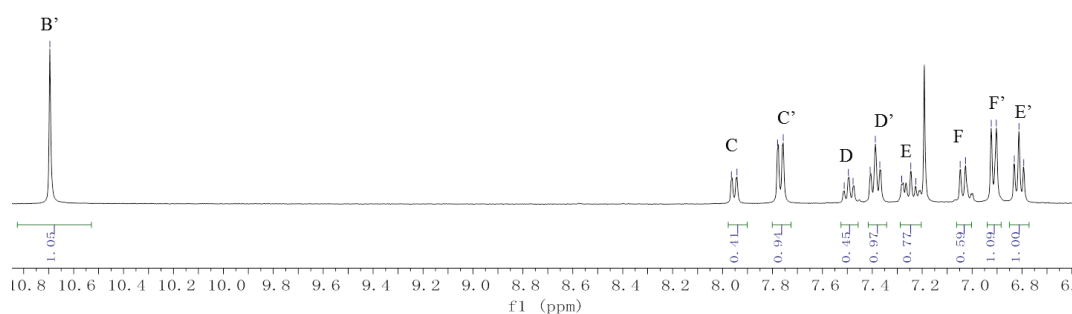
Supplementary Figure 14 | ¹H NMR spectra of aspirin methyl ester (AME) and the product of AME hydrolysis by Lipase@ZIF-8.



Supplementary Figure 15 | ¹H NMR spectra of aspirin methyl ester (AME) and the product of AME hydrolysis by Lipase@MCM-41.

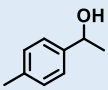
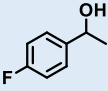
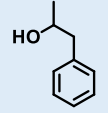


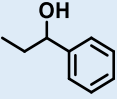
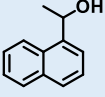
Conversion rate=4/6.22=64.31%

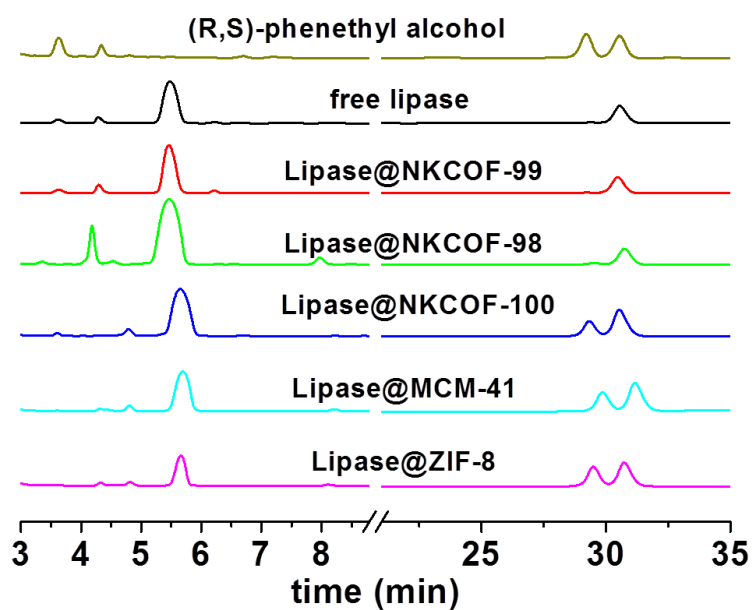


Supplementary Figure 16 | ^1H NMR spectra of aspirin methyl ester (AME) and the product of AME hydrolysis by Lipase@NKCOF-100.

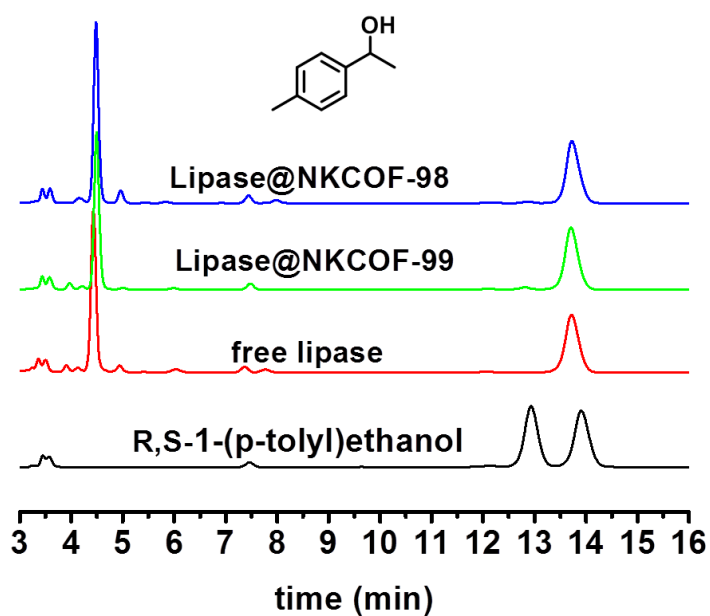
Supplementary Table 1 | Analytical conditions.

Racemic alcohol	Mobile Phase (v/v)	Current Speed (mL/min)	Detection Wavelength (nm)
	n-hexane /isopropanol		
	97/3	1.0	254
	97/3	1.0	254
	97/3	1.0	254
	n-hexane/MeOH /EtOH		

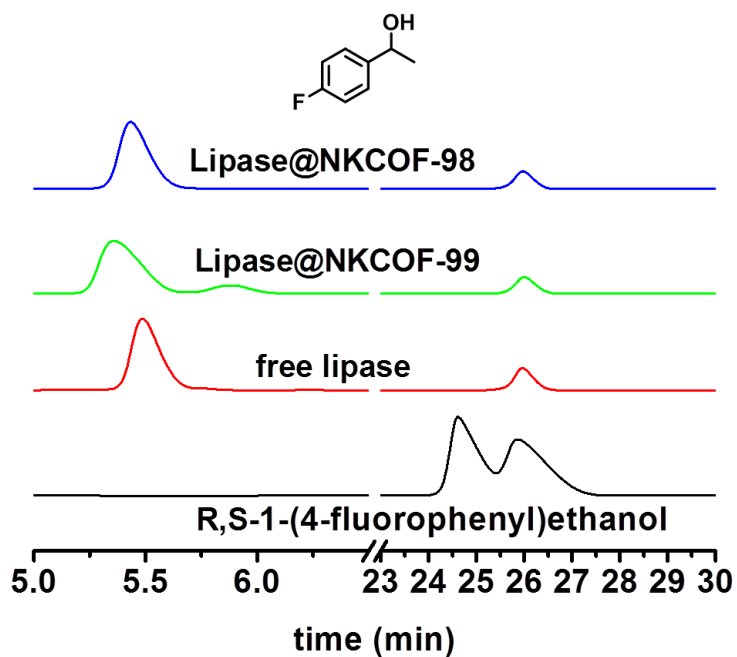
	99/0.5/0.5	1.0	254
	99/0.5/0.5	1.0	254



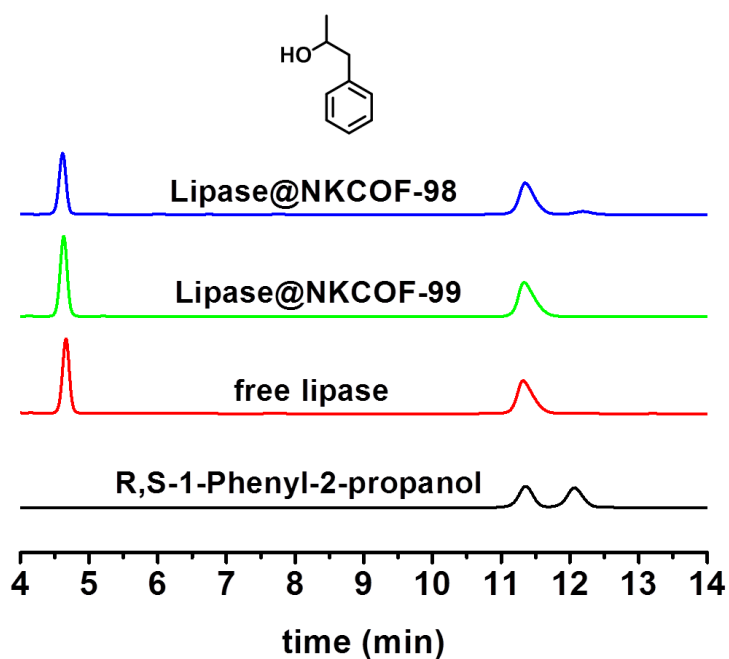
Supplementary Figure 17 | Catalytic reaction results (HPLC) of various Lipase@materials in the period of 12 h.



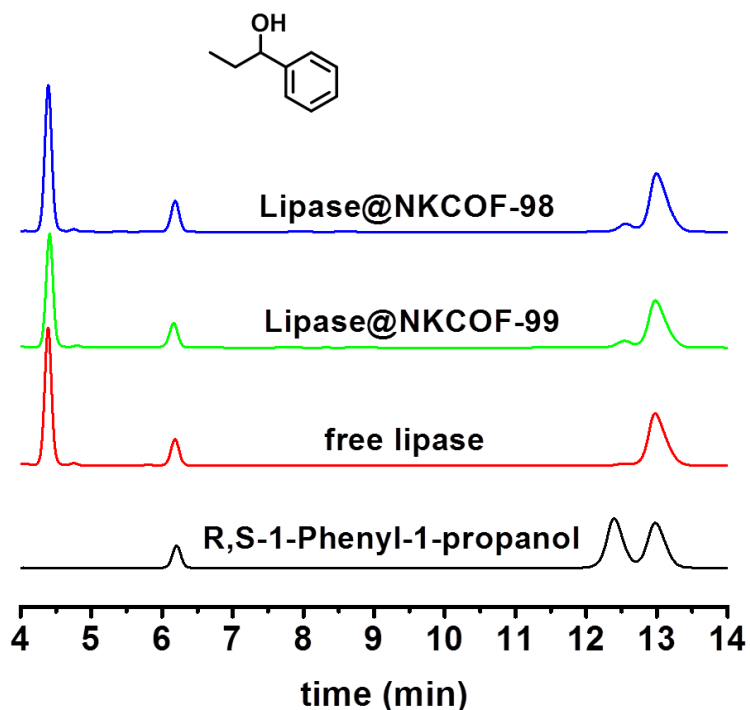
Supplementary Figure 18 | Catalytic reaction results (HPLC) of free lipase, Lipase@NKCOF-98 and Lipase@NKCOF-99 in chiral resolution of R, S-1-(p-tolyl)ethanol.



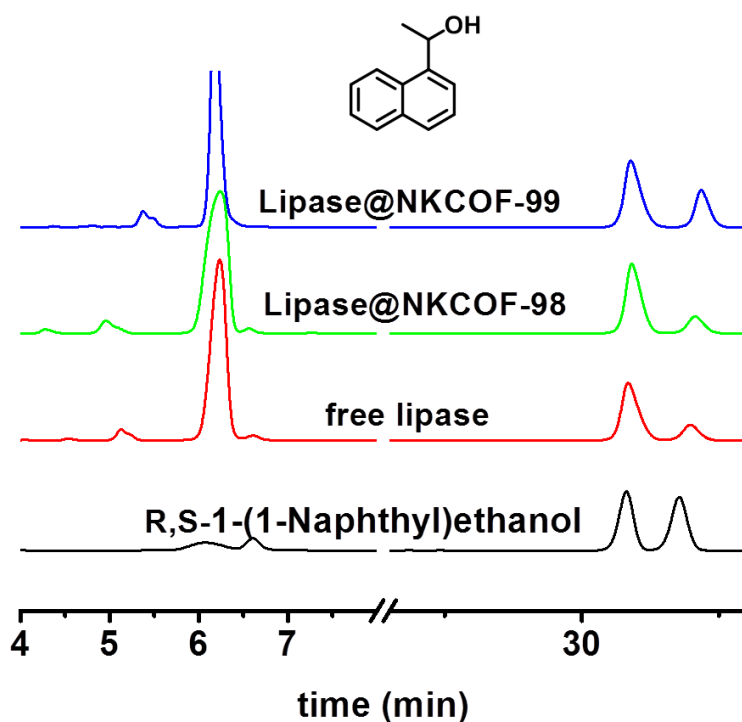
Supplementary Figure 19 | Catalytic reaction results (HPLC) of free lipase, Lipase@NKCOF-98 and Lipase@NKCOF-99 in chiral resolution of R, S-1-(4-fluorophenyl)ethanol.



Supplementary Figure 20 | Catalytic reaction results (HPLC) of free lipase, Lipase@NKCOF-98 and Lipase@NKCOF-99 in chiral resolution of R, S-1-Phenyl-2-propanol.



Supplementary Figure 21 | Catalytic reaction results (HPLC) of free lipase, Lipase@NKCOF-98 and Lipase@NKCOF-99 in chiral resolution of R, S-1-Phenyl-1-propanol.



Supplementary Figure 22 | Catalytic reaction results (HPLC) of free lipase, Lipase@NKCOF-98 and Lipase@NKCOF-99 in chiral resolution of R, S-1-(1-Naphthyl) ethanol.